IEEE Access
Multidisciplinary ⋮ Rapid Review ⋮ Open Access Journal

Received 28 June 2022, accepted 23 July 2022, date of publication 4 August 2022, date of current version 11 August 2022.

Digital Object Identifier 10.1109/ACCESS.2022.3196473

APPLIED RESEARCH

Posture Risk Assessment in an Automotive Assembly Line Using Inertial Sensors

MARIA LUA NUNES[1,2], DUARTE FOLGADO[1,3], CARLOS FUJÃO[4], LUÍS SILVA[3], JOÃO RODRIGUES[3], PEDRO MATIAS[1], MARÍLIA BARANDAS[1,3], ANDRÉ V. CARREIRO[1], SARA MADEIRA[5], AND HUGO GAMBOA[1,3], (Senior Member, IEEE)

[1]Associação Fraunhofer Portugal Research, 4200-135 Porto, Portugal
[2]Department of Physics, Biomedical and Biophysics Engineering, Faculty of Sciences of the University of Lisbon, 1749-016 Lisbon, Portugal
[3]FCT NOVA Laboratory for Instrumentation, Biomedical Engineering and Radiation Physics, NOVA University of Lisbon, Lisbon, 2829-516 Caparica, Portugal
[4]Industrial Engineering & Production System (Ergonomics Team), Volkswagen Autoeuropa, Quinta do Anjo, 2954-024 Palmela, Portugal
[5]Department of Informatics, Data Science, Faculty of Sciences of the University of Lisbon, 1749-016 Lisbon, Portugal

Corresponding author: Maria Lua Nunes (maria.nunes@fraunhofer.pt)

This work was supported in part by the European Regional Development Fund (ERDF) through the North Portugal Regional Operational Program and Lisbon Regional Operational Program under Grant NORTE-01-0247-FEDER-045910, and in part by the Portuguese Foundation for Science and Technology under the Massachusetts Institute of Technology (MIT) Portugal Program (2019 Open Call for Flagship projects).

This work involved human subjects or animals in its research. Approval of all ethical and experimental procedures and protocols was granted by the Ethics Committee of the Faculty of Psychology and Educational Sciences of the University of Porto (FPCEUP), and performed in line with the Declaration of Helsinki.

ABSTRACT Musculoskeletal disorders (MSD) are a highly prevalent work-related health problem. Biomechanical exposure to hazardous postures during work is a risk factor for the development of MSD. This study focused on developing an inertial sensor-based approach to evaluate posture in industrial contexts, particularly in automotive assembly lines. The analysis was divided into two stages: 1) a comparative study of joint angles calculated during movements of the upper body segments using the proposed motion tracking framework and the ones provided by a state-of-the-art inertial motion capture system and 2) a work-related posture risk evaluation of operators working in an automative assembly line. For the comparative study, we selected data collected in laboratory (N = 8 participants) and assembly line settings (N = 9 participants), while for the work-related posture risk evaluation, we only considered data acquired within the automotive assembly line. The results revealed that the proposed framework could be applied to track industrial tasks movements performed on the sagittal plane, and the posture evaluation uncovered posture risk differences among different operators that are not considered in traditional posture risk assessment instruments.

INDEX TERMS Inertial sensors, ergonomics, motion analysis.

I. INTRODUCTION

Musculoskeletal Disorders (MSD) are the most prevalent work-related health problem among European Union workers, with three out of five workers reporting MSD complaints, mainly about the upper body [1]. These numbers represent a primary concern worldwide, not only due to the pain and disability suffered by the worker, but also to its economic impact on the employer and society [2]. Effective management of work-related health requires the management of both sickness absence and presence by controlling exposure risk factors [3]. Work-related MSD (WRMSD) risk factors can be classified into personal (e.g., medical history) or related to the workplace (i.e., physical and psychosocial work environment) [4].

There are three main types of methods to assess occupational risk [5], [6]: self-reported, observational, and directly-measured. In the first, the risk is perceived by the worker, e.g., throughout questionnaires and interviews, which can be unreliable as it depends on the worker's literacy and risk exposure perception. The observational method is conducted by ergonomic experts and is based on instruments

The associate editor coordinating the review of this manuscript and approving it for publication was Kang Li.

(e.g., checklists), standards, and guidelines. It can be a demanding and time-consuming task for ergonomic teams, with limited observation time and mostly qualitative. The directly-measured methods use sensors to capture the workers' motion and activity, providing relevant data for the occupational risk assessment. However, in practice, only self-reported and observational approaches are conducted on a more frequent basis [7].

Moreover, note that risk assessment instruments used by ergonomic experts, such as the European Assembly Worksheet (EAWS) [8], guidelines and standards, derive from risk factors specifications provided by epidemiological studies, e.g. [9], [10]. Hence, ergonomic intervention approaches designed for WRMSD prevention that rely on these instruments' outcomes are well-founded.

While exploring key enabling technologies towards human-automation symbiosis work systems, the authors of [11] introduce the concept of the ''Operator 4.0''. Among other technologies, the ''Operator 4.0'' proposes the usage of wearable motion capture (MoCap) technology throughout ubiquitous data collection, enabling an objective risk assessment.

The majority of MoCap systems exploited in industrial contexts research are based on Inertial Measurement Unit (IMU) sensors rigidly attached to human body segments [12]. Nonetheless, the inertial sensing technique still lags in sensor durability, information validity and efficacy, and worker's compliance [13]. Yet, a recent study with 31 participants, conducted by [14] in a manufacturing working environment, concluded that operators report low ratings of discomfort, distraction, and burden while wearing inertial devices during work.

Directly-measured methods used to quantify the risk exposure resort to information about segments' orientations and joint angles. These data can be derived from on-body inertial sensors setups, which collect body segments acceleration, rotation, and magnetic field data used on motion reconstruction algorithms based on sensor fusion techniques [15], [16]. Inertial MoCap data has often been validated within laboratory settings using optical MoCap data as ground truth [17]–[22]. However, in industrial shop floor, existing ferromagnetic interferences disturb inertial sensors data, subsequently degrading the orientation estimates. There are fewer research works on the assessment of estimates based on data acquired in real industrial settings. The usage of an optical MoCap to validate segments orientation and joint angles calculated using inertial data, acquired in real industrial settings, can be challenging due to the marker occlusions which prevents the optical MoCap motion reconstruction [12]. Inertial systems developed by Xsens have been extensively validated with optical MoCap systems in laboratory settings. Furthermore, according to Xsens, these feature compensation mechanisms to mitigate magnetic disturbances and drift, being used in recent studies without the need for validation with an optical MoCap system [23].

Over workplace ergonomics research, several methods have been pursued to analyze human motion data acquired in occupational settings [13], which provide outputs to assess postural biomechanical exposure and the resulting risk. Descriptive statistics methods use the median, mean, standard deviation, range and percentiles, as measures of exposure that are selected considering risk factors specifications and calculated either for the entire acquisition duration or stratified by condition for comparison (e.g., by job category, task types) [24], [25]. In addition, inferential statistic methods, such as ANOVA or mixed effects analysis, have been undertaken to establish relationship variables among measurements of occupational exposure [26], [27]. Moreover, several studies provided computational implementations of the Rapid Upper Limb Assessment (RULA) instrument, using statistical measures and assessing upper body posture risk within real-world settings [20], [21], [28]–[30].

Other methods rely on applying more sophisticated data mining algorithms on human motion data. The authors of [31], [32] proposed a time series similarity measurement that can be used to quantify the operators' distance to a standard work method. Furthermore, the analysis of time series regarding human motion data is often complemented using feature-based representations of the resulting signals. These feature-based representations have been used to discover undefined and seemingly featureless patterns in data to characterize industrial processes. Examples of features are inertial and orientation data [20], [33]–[38], data-related statistical measurements [37], [39]–[41] and metrics derived from the application of risk assessment instruments [42], [43].

Despite current well-founded risk assessment approaches using direct measuring, there are barriers to their adoption in large manufacturing settings. Therefore, it is necessary to continue researching how to automate data collection and processing to engage traditional and innovative methods to improve the existing risk evaluation.

There has been an increased interest in developing directly-measured methods in the last few years. However, studies usually validate their approaches only based on laboratory protocols that simulate work processes [44]. Few studies validated MoCap systems when tracking operators' motions in real industrial contexts and compared the motion tracking performance when moving from controlled (i.e, laboratory) to uncontrolled settings (i.e, real industrial context). Additionally, very few studies established a relationship between biomechanical exposure and resulting risk over work-cycle data, such as the authors of [45], or compared different operators' work method. These analyses could provide relevant information to industrial processes redesign and adjustments, perceiving high-risk tasks, and increased exposure.

In [21] we validated our proposed inertial on-body sensors network within laboratory settings using an optical MoCap (i.e, VICON). Hence, we considered the inertial data provided by our sensors accurate in the laboratory environment. In the

present study, we extend our prior work with an improved inertial MoCap framework in order to estimate joint angles, concerning movements of the upper body segments on the sagittal plane (i.e, flexion/extension). Further, the goal was to apply those methods to track human motion in real industrial settings. We also propose a computational implementation of a section of the risk assessment instrument EAWS in order to evaluate the work-related posture risk. Beyond the methods, the main contributions of this work include the following:

1) Comparison of the joint angles calculated using the proposed framework and provided by a state-of-the-art validated inertial MoCap;
2) Evaluation of work-related posture risk with respect to a case study in an automotive assembly line.

Our previous study [21] and the current study differ in the motion reconstruction algorithm (the latter proposes an automatic data-driven synchronization method and an angular extraction approach based on kinematics descriptions) and in the ergonomic risk assessment instrument implemented.

The rest of this paper is structured as follows: Section II describes the materials used and methods developed, including the MoCap routine and motion tracking framework, and the computational implementation of EAWS instrument. Then, Section III discusses the obtained results. Finally, Section IV presents the main conclusions and future research outlook.

II. MATERIALS AND METHODS

An automotive assembly line is divided into diverse processes, from parts production and rendering to their assemblage. Among the different processes needed to produce a car, manual processes are the ones that could compromise workers' health and safety. For our case study, we selected the fitting processes. As vehicles are assembled, the fit-up of various parts is inspected by measuring the width of the gap between adjacent panels and the alignment of surfaces. After checking the need for fitting on each car, workers perform adjustments until the reference condition is achieved. Some examples of panels composing a vehicle are depicted in Fig. 1.

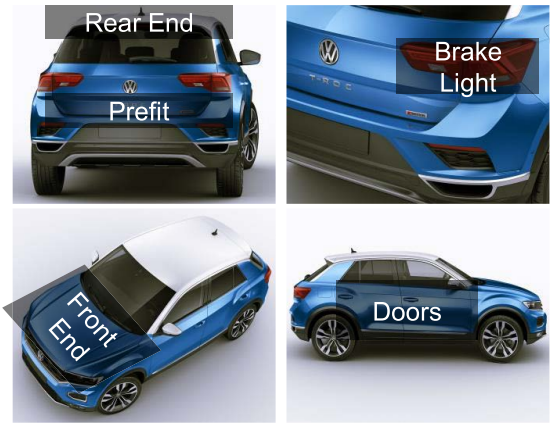

FIGURE 1. Examples of car panels that are verified and aligned during fitting processes.

Our study results were divided into two stages: 1) comparison of calculated joint angles with *equivalent* data provided by a state-of-the-art inertial MoCap; and 2) work-related posture risk evaluation.

The comparison aimed to assess the reliability of the motion tracking for upper body segments movements on the sagittal plane, i.e., spine, shoulders, elbows, and wrists joints flexion/extension angles. Accordingly, the data estimated, using our proposed inertial MoCap routine and the developed framework were compared with the data provided by a Xsens' system.

We consider that both systems can be prone to magnetic disturbances and drift since there is a lack of studies validating the Xsens' system under highly ferromagnetic environments, such as an automotive assembly line. Hence, our comparison aims to assess the consistency between our proposed system and the Xsens' system data in laboratory and real industrial settings.

At the risk evaluation, we analyzed the biomechanical exposure and resulting risk, both at the workstation- and operator-level. This allowed us to compare the risk assessment outputs among different workstations and workers in the selected case study. Furthermore, we computed the biomechanical exposure and resulting risk using joint angles provided by the Xsens' system and determined the mean and standard deviation of absolute differences between Xsens' system and our system posture evaluation results.

It should be noticed that the data acquired in the laboratory were exclusively used for the reliability assessment (i.e, joint angles comparison), while the automotive assembly line data were handled for both joint angles comparison and evaluation. As follows, the risk assessment was only conducted on automotive assembly line data.

A. DATA COLLECTION

1) SYSTEM SETUP

We simultaneously used the two inertial MoCap systems as depicted in Fig. 2.

The proposed on-body inertial sensor network comprises seven wireless Kallisto IMUs (Sensry Gmbh, Dresden, Germany), collecting data at 100 Hz. The other inertial system considered for our study was the MVN Awinda (Xsens, Enschede, Netherlands), collecting data at 60 Hz.

The IMUs from our proposed setup were attached to the subjects' bodies as follows: one IMU inside a glove for each hand, one IMU for each upper arm, and forearm using velcro straps; and one IMU for the trunk fixed to a waistcoat and located on the chest. Each sensor was placed with the x-axis of the sensor frame along the longitudinal axis of the respective body segment, pointing from distal to proximal extremity, and with the z-axis normal to the segment, as depicted in Fig. 3. The MVN Awinda IMUs were attached according to the full-body motion tracking guidelines [46].

(a) Chest

(b) Upper Arm

(c) Forearm and Hand

FIGURE 2. Placement setups of the two inertial MoCap systems.

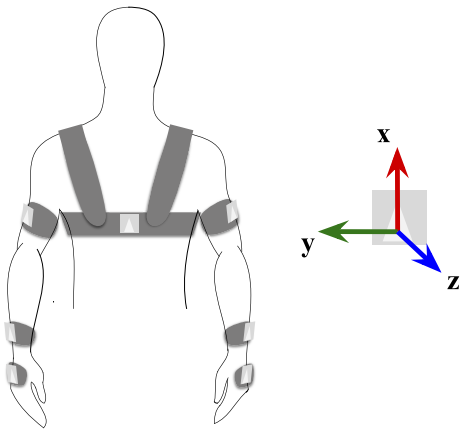

FIGURE 3. An illustrative figure detailing our proposed on-body inertial sensors network setup.

The joint motion reconstruction using the proposed on-body inertial sensor network data was performed using the motion tracking framework, further described in section II-B. The MVN Awinda setup relied on the MVN Analyze to record and extract joint angles data. This data was transformed to match the joint angles computed using the developed motion tracking framework.

Additionally, we also collected video recording data to provide a visual reference for additional post-acquisition inspection.

The data collected in the assembly line were annotated with the timestamps corresponding to the beginning and end of each work-cycle (5 ± 2 cycles per acquisition). The annotation was performed using the NOVA software [47].

2) PROTOCOLS

The laboratory and automotive assembly line (assembly line will be referred to as field) data collection protocols differed since they had separate goals. Nevertheless, both protocols included collecting each participant's body measurements, both systems calibrations, and synchronization procedures.

There were two stages of our system calibration: 1) hardware and 2) model calibrations. The former consists of calibrating our IMUs within the data collection environment. To control data quality, a visual inspection of each IMU's signals and, further, sampling frequency verification were conducted. To calibrate the model, subjects were asked to maintain the neutral pose for 15 seconds. The subject's posture during the calibration was then matched to the default pose of the biomechanical model used.

The Xsens' system only required model calibration, conducted according to the guidelines [46].

Aiming to define a common temporal reference within sensors and between systems, we asked the subjects to perform a purposeful preset movement at the beginning and end of each acquisition. We used that movement to conduct a data-driven temporal synchronization. Movement and synchronization method are described in section II-B2.

The following tasks were tracked according to each setting:

- Laboratory: each participant was asked to perform five trials - two functional trials, where each subject mobilized his/her upper limbs (for approximately 5 minutes) and trunk (for approximately 2 minutes) joints degrees of freedom (DoF) within their respective ranges of motion (RoM); and three goal-oriented sets (approximately 2 minutes each), wherein specific tasks were given to the participants. The latter were named simulation trials, as they simulate real operation tasks composing the fitting processes and required the use of tools within safety limits.
- Field: each worker was tracked between 15 to 50 minutes conducting regular work, namely fitting car panels highlighten in Fig. 1.

3) PARTICIPANTS

Seventeen participants (Tables 1 and 2) were recruited into this study: eight and nine subjects cooperated in the laboratory and automotive assembly plant acquisitions, correspondingly. The study population was purposive, i.e., volunteer participants within the scope of the study, and was formed by Portuguese citizens. Thus, the sample is geographically and culturally limited. Volunteers were asked if the occupational doctor had assigned any medical restrictions. If not, they were considered "healthy" and took part in the study sample, being excluded otherwise. Informed consent was signed to respect

TABLE 1. Laboratory population characteristics and protocol tasks. Classes of body profiles are small (S), medium (M) and high (H).

ID	Age (range of years old)	Gender	Task (Protocol)	Body Profile (class)
Subject 1	[20, 30[	M	Functionals + Simulation	H
Subject 2	[20, 30[	M	Functionals + Simulation	M
Subject 3	[30, 40[	F	Functionals + Simulation	S
Subject 4	[30, 40[	M	Functionals + Simulation	M
Subject 5	[20, 30[	M	Functionals + Simulation	M
Subject 6	[20, 30[	F	Functionals + Simulation	S
Subject 7	[20, 30[	M	Functionals + Simulation	S
Subject 8	[20, 30[	M	Functionals + Simulation	M

TABLE 2. Field population characteristics and protocol tasks. Classes of body profiles are small (S), medium (M) and high (H).

ID	Age (range of years old)	Gender	Task (Protocol)	Body Profile (class)
Operator 1	[30, 40[	M	*Doors* Right *Doors* Left	H
Operator 2	[30, 40[	M	*Doors* Right *Doors* Left	M
Operator 3	[30, 40[	M	*Doors* Right *Prefit*	M
Operator 4	[30, 40[	M	*Brake Light* Right *Brake Light* Left *Rear End* *Front End*	H
Operator 5	[30, 40[	M	*Prefit* *Brake Light* Right *Brake Light* Left *Rear End* *Front End*	S
Operator 6	[40, 50[	M	*Doors* Right *Doors* Left *Prefit*	M
Operator 7	[40, 50[	M	*Brake Light* Right *Brake Light* Left *Rear End* *Front End*	M
Operator 8	[40, 50[	M	*Brake Light* Right *Brake Light* Left *Rear End* *Front End*	M
Operator 9	[40, 50[	M	*Brake Light* Right *Brake Light* Left *Rear End* *Front End*	M

each participant's privacy and inform them precisely what would be done with their data.

Tables 1 and 2 shows laboratory and field data collections samples characteristics. Note that participants' ages are distributed in three ranges: [20, 30[, [30, 40[and [40, 50[years old. The body measurements distributions percentiles are displayed in Table 3. Participants' body profiles classes were defined based on their height (178 $\pm$ 10 cm), body mass (75 $\pm$ 14 kg), arm span (175 $\pm$ 9 cm), shoulder width (40 $\pm$ 4 cm), hip height (100 $\pm$ 8 cm), knee height (53 $\pm$ 4 cm), ankle height (11 $\pm$ 1 cm) and shoe size (30 $\pm$ 2 cm). For each body measurement, we observed if its value was below 25% percentile (small), between 25% and 75% percentiles (medium) or above 75% percentile (high) in relation to the study population. The class of a participant's body profile was defined according to the most frequent classification among the participant's body measurements, as small (S), medium (M), or high (H).

TABLE 3. Population characteristics distribution percentiles per body measurement collected.

	Percentile (%)		
	75	50	25
Height (cm)	184	176	170
Weight (kg)	82	77	65
Hip height (cm)	105	100	95
Arm span (cm)	183	171	166
Ankle height (cm)	12	11	10
Knee height (cm)	55	53	49
Shoulder width (cm)	43	39	37
Shoe size (cm)	31	30	27

B. MOTION TRACKING FRAMEWORK

In the following sections, we will present the proposed motion tracking framework. Only the IMU data acquired using the proposed on-body sensor network underwent the motion tracking framework. We focused its application on the spine, shoulders, elbows, and wrists joints' flexion/extension DoFs.

1) DATA PREPROCESSING

The on-body sensor network signals were linearly resampled to 100 Hz. The accelerometer and magnetometer signals were filtered using a 4th order Butterworth low-pass filter with a cutoff frequency of 10 Hz [48], [49]. The gyroscope was filtered with a 4th order Savitzky-Golay polynomial filter with a window size of 11 samples [50].

2) DATA SYNCHRONIZATION

Our on-body sensor network does not have a communication protocol to synchronize the multiple sensors. As previously mentioned in section II-A2, the data collection protocol had a purposeful preset movement that all subjects performed before and after the acquisition to synchronize data from IMUs placed in different segments. The movement consisted of performing a vertical jump.

The algorithm developed to synchronize data streams from the multiple sensors is summarized in Fig. 4. The algorithm uses peak detection methods to identify synchronization opportunities from signals collected from different sensors. The synchronization opportunities **O** are filtered using a technique to identify pairwise correspondences. The final matches are named as alignment points **A**. An alignment point is a representation of a physical event in a sensor data stream that can be accurately distinguished and directly related to the same event in the data stream of another sensor (i.e., coupling occurrence) [51]. In our case, the physical event of interest was the vertical jump.

The Xsens' system uses a communication protocol to synchronize its multiple sensors.

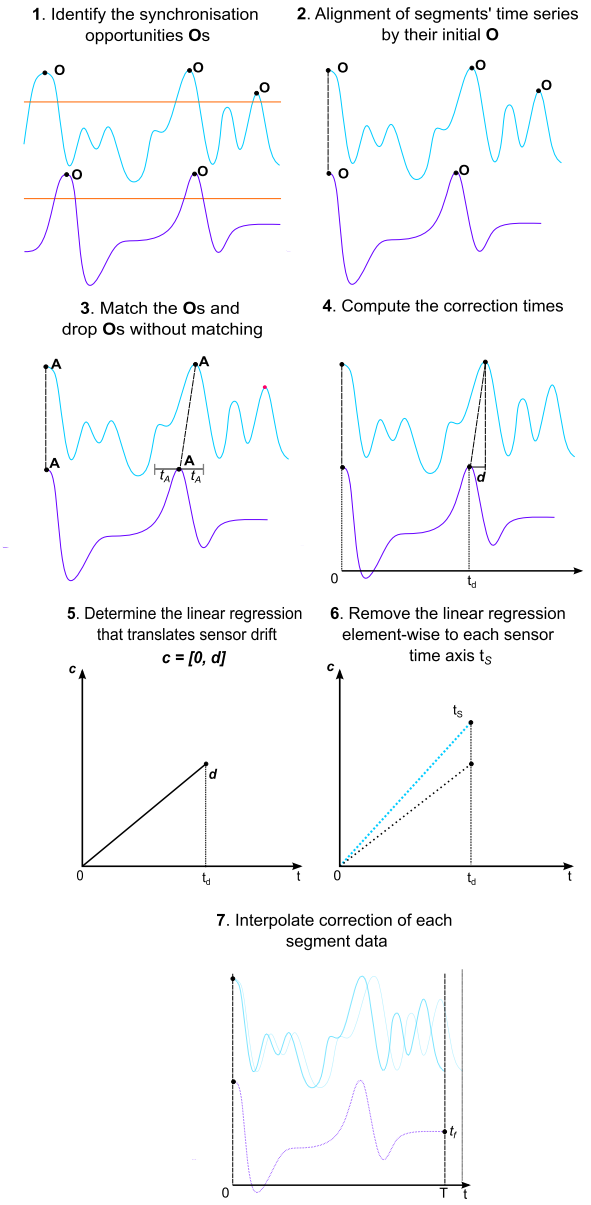

FIGURE 4. A stepwise description of the temporal synchronization algorithm. (1) Synchronization opportunity (O) events are identified using peak detection method. (2) For each sensor data streams (x-, y- and z-axis acceleration, magnetic field and angular velocity data), samples with an index anterior to the first O index are cut off. (3) Match the remaining synchronization opportunity events between different sensors, if their distance in time is less than the maximum interval (t_A, where A refers to alignment point). (4) For each sensor, compute the vector of differences in time between the occurrence of each alignment point in sensor data and in another sensor data, selected as reference, - the correction intervals (c) - and (5) determine the linear regression that describes c (which models the sensor desynchronization). (6) Desynchronization is eliminated by subtracting c to the sensor time (t_S). (7) Interpolate all sensors to a common temporal reference.

3) ATTITUDE ESTIMATION

Attitude estimation was conducted using the nine DoF Madgwick filter implementation provided by the AHRS: Attitude and Heading Reference Systems open-source python toolbox [52]; it uses x-, y- and z-axis acceleration, magnetic field and angular velocity data for each sensor attitude estimation.

TABLE 4. Upper body segments joints' flexion/extension DoF and the respective RoM, defined according to the model [55].

Segment	DoF	RoM
Trunk	Lumbar flexion/extension	[-90°, 90°]
Upper arm	Upper arm extension/flexion	[-90°, 180°]
Forearm	Elbow extension/flexion	[0°, 160°]
Hand	Wrist extension/flexion	[-90°, 90°]

Madgwick filter is a sensor fusion algorithm that enables a fair orientation estimation performance at low sampling rated data and compensation of magnetometer magnetic distortion. Additionally, it also enables to compensate gyroscope low-frequency bias (i.e. drift) [53].

The filter provides the attitude representation of each IMU in regards to the Earth's reference frame in the East-North-Up (ENU) convention, which will be needed to the inverse kinematics (described in section II-B4).

The attitude is represented as a quaternion that is a 4-dimensional complex number defined as the sum of a scalar q_0 and a vector $\mathbf{q} = (q_1, q_2, q_3)$ [54]. Accordingly, the quaternion representation can be used to characterize a rotation of a segment frame about an axis, defined in 3-dimensional space.

4) INVERSE KINEMATICS

Inverse kinematics (IK) provides insight into measured movement and was performed through the OpenSim software's OpenSense workflow [17].

The IMUs orientation data, resulting from methods described in section II-B3, were imported and assigned to a biomechanical model.

In model calibration, we used the calibration pose data to place and establish the orientation of each IMU on the corresponding body segment in the model (i.e, model's virtual IMU); and we considered the chest IMU as the base IMU, i.e., the IMU representing the model's segment from which other segments move as a chain.

According to the authors of [17], OpenSense workflow IK corrects segments orientations and calculates joint angles considering model joints kinematics descriptions. It solves an optimization problem minimizing the difference between the experimentally measured IMUs orientations expressed in the Earth's reference frame and the orientations of the model's virtual IMUs.

We used the full human body model developed by [55]. It is less detailed about the motion of the upper body region than other models, such as [56]–[58], but the information retrieved by the model was adequate for this research, presenting lower computational complexity and resorting to simpler joints motion definitions.

Table 4 summarizes the flexion/extension DoF and respective RoM of segments, defined according to the model [55].

C. STATISTICAL ANALYSIS

A statistical analysis was performed to compare joint angles data retrieved by the systems. We assessed the consistency

and agreement between data estimated using our motion tracking framework and data provided by the Xsens' system in both laboratory and field data collections.

Consistency definition concerns the degree to which the estimated data (y) is related to the data provided by Xsens' system (x) plus a systematic error (c) (ie, $y = x + c$). We considered c as the unknown differences between the joints' kinematic descriptions of the biomechanical model selected and the one used by Xsens. Intraclass correlation coefficient (ICC) estimates and their 95% confidence intervals (CI) were calculated using *rpy2* python package based on a mean-measurement (n = 100 measurements per acquisition), consistency, 2-way mixed-effects model. ICC was calculated for each upper body joint flexion/extension DoF data, and both laboratory and automotive assembly plant settings. The authors of [59] proposed that ICC values less than 0.5 are indicative of poor reliability; between 0.5 and 0.75 indicate moderate reliability; between 0.75 and 0.9 indicate good reliability; and greater than 0.90 indicate excellent reliability.

Standard error of measurement (SEM) values were also calculated. SEM was selected as an indicator of absolute reliability of measurement [60].

D. AUTOMATED RISK ASSESSMENT

The EAWS is a risk assessment instrument to estimate risk exposure by computing a total risk score. This score combines partial scores from posture, strength, force, and repetition. This instrument is originally based on the observation of workstation and work method. We developed an automated approach to estimate partial scores for upper body segments postures on their sagittal plane.

Fig. 5 is an excerpt from the EAWS showing the rating scales of partial risk scores relative to basic postures and movements of the trunk and arms. The partial risk score depends on the work-cycle time in the posture, i.e., its biomechanical exposure, and on its rating scale. For example, if an operator is 5 % of the work-cycle upright and with hands above head level, the partial risk score is 5,3 points. These scores are calculated automatically using our proposed approach, excluding the components of shoulders abduction that could increase scores about the two last lines (in Fig. 5 EAWS section). Notice that we consider the exposure to a posture as the relative frequency of the posture's occurrence in a work-cycle, excluding the analysis of time spent in the posture in terms of duration of posture's occurrence.

It is worth emphasizing that a complete EAWS evaluation has additional sections whose variables cannot be directly quantified using an inertial sensor setup, such as the force and loads.

Moreover, this study focused on the sagittal plane due to the priority on studying joints' flexion/extension. Nonetheless, there are sections addressing postures concerning the upper body segments movements on the coronal and transverse planes.

Fig. 6 contains a stepwise description of the implemented procedure until the risk assessment. Firstly, each work-cycle

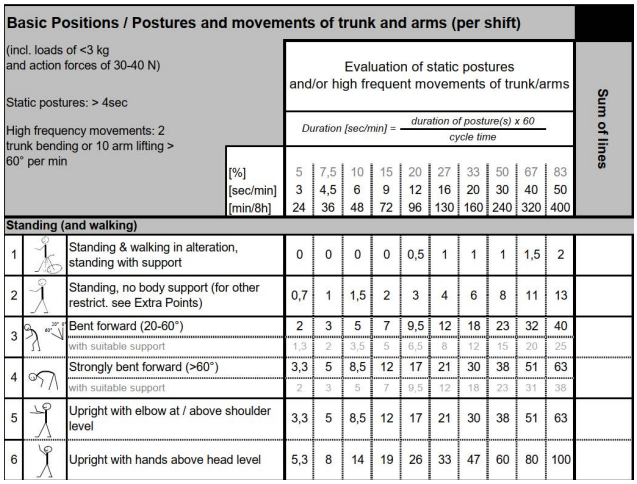

FIGURE 5. Excerpt of EAWS - Basic positions/postures and movements of trunk and arms - standing (and walking) section.

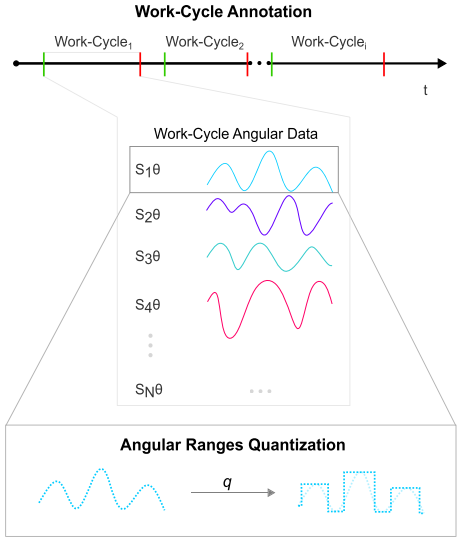

FIGURE 6. Work-cycles annotation performed in data from an acquisition. Work-cycle angular data is a set of time series, one for each segment's S_N flexion/extension DoF, θ, where N varies from 1-7. Angular ranges quantization: a function q was implemented for each segment flexion/extension DoF, as described in Fig. 7.

angular data were downsampled to 1 Hz. Secondly, the data were quantized according to the working postures described in EAWS.

A diagram of conditions used to assign joint angles to angular ranges related to EAWS postures (selected to risk assessment) is shown in Fig. 7. The conditions were chosen taking into consideration feedback from two ergonomists that supported our study. The joint angles used as input were flexion/extension DoF of the trunk (1), upper arms (1 DoFs × 2 arms = 2 DoFs) and forearms (1 DoFs × 2 arms = 2 DoFs) segments (see Table 4).

Furthermore, the angular ranges data were taken as input to the biomechanical exposure determination. The biomechanical exposure consists of the percentage of values in

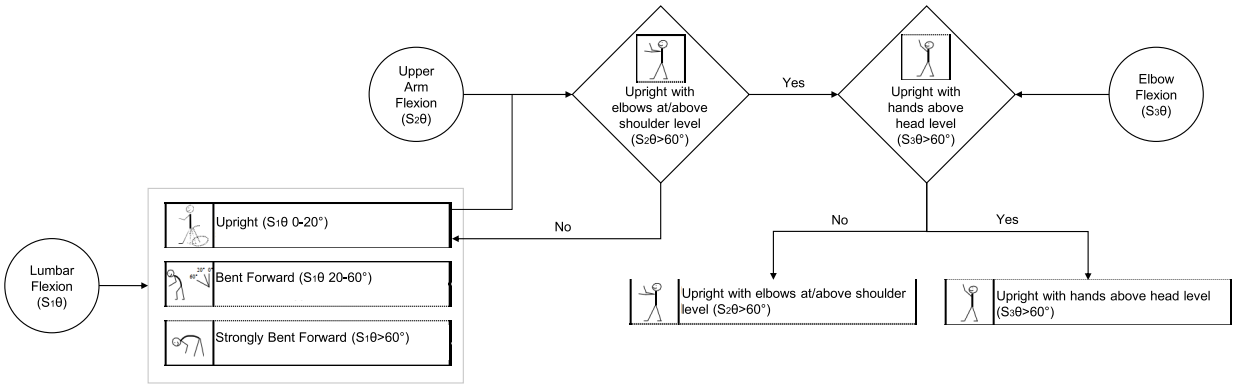

FIGURE 7. Conditions defining the EAWS postures selected to risk assessment. Firstly, the lumbar flexion/extension data is divided into three angular ranges - "Upright", "Bent Forward" and "Strongly Bent Forward". Afterwards, it is verified if there is data within the "Upright" angular range that also verifies the "Upright with elbows at/above shoulder level condition"; if so, data is assign to that angular range and removed from "Upright" data. Finally, it is verified if there is data within the "Upright with elbows at/above shoulder level condition" angular range that also verifies the "Upright with hands above head level"; if so, data is assign to that angular range and removed from "Upright with elbows at/above shoulder level condition" data.

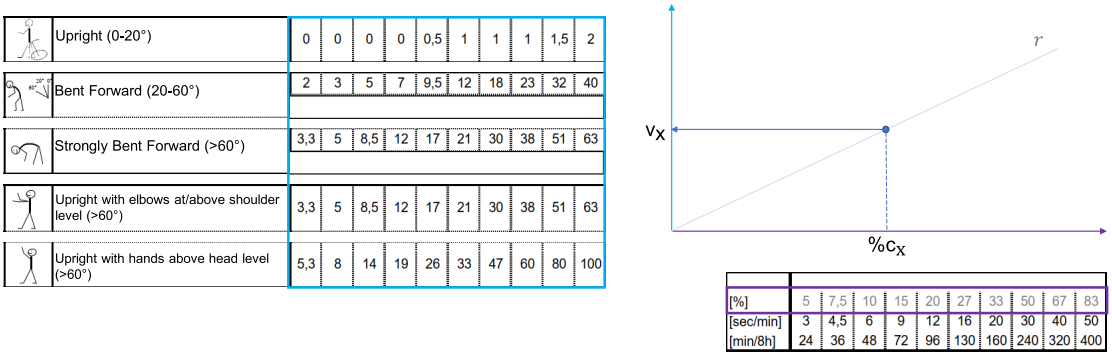

Upright (0-20°)	0	0	0	0	0,5	1	1	1	1,5	2
Bent Forward (20-60°)	2	3	5	7	9,5	12	18	23	32	40
Strongly Bent Forward (>60°)	3,3	5	8,5	12	17	21	30	38	51	63
Upright with elbows at/above shoulder level (>60°)	3,3	5	8,5	12	17	21	30	38	51	63
Upright with hands above head level (>60°)	5,3	8	14	19	26	33	47	60	80	100

[%]	5	7,5	10	15	20	27	33	50	67	83
[sec/min]	3	4,5	6	9	12	16	20	30	40	50
[min/8h]	24	36	48	72	96	130	160	240	320	400

FIGURE 8. Biomechanical exposure (i.e, percentage of work-cycle time in each posture) is determined and the respective partial risk score is calculated using the linear regression, constructed according to EAWS instrument rating scale. c_X and v_X denote the biomechanical exposure and risk score related to each posture, respectively.

each posture X ($\%c_X$) per work-cycle. We used EAWS rating scales to draw linear regressions of partial risk scores (r) as a result of biomechanical exposures (see Fig. 8). Thus, for each posture, the biomechanical exposure was determined, and the respective partial risk score (v_X) was computed using the linear regression.

The total risk score was also calculated as the sum of the postures' partial risk scores. Note that, for the postures of the upper limbs, only the highest sum value, assigned either to the right or to the left limb, was considered in the final total risk score sum.

III. RESULTS AND DISCUSSION

A. JOINT ANGLES COMPARISON

Table 5 shows the values of ICC, the respective 95% IC and SEM.

Regarding laboratory results, ICC values, and the respective 95 % CIs, shows that the tracking of flexion/extension movements from elbows is excellent; spine, shoulders, and left wrist are good; and right wrist is moderate to good. Nonetheless, shoulders SEMs are greater than 10°.

Field results highly decreased in consistency and agreement when compared to the laboratory setting. Spine and elbows estimates are moderately consistent with Xsens' system data, while shoulders decrease for poor to moderate and wrists to poor. The SEMs are steadily higher than 10° for every joint.

The higher SEM values for shoulders flexion/extension in laboratory and field settings could be due to increased soft tissue artifact (STA) occurrence, i.e., the skin motion relative to the underlying bone, which is the primary source of error in inertial motion tracking [61], [62].

Additionally, an initial offset between the participant's body calibration posture and the biomechanical model's default pose can introduce error into angular estimates. For instance, when a body segment is close to an extreme posture, the estimation might result in an impossible segment's posture according to the model, which is then wrongly adjusted by the algorithm. Moreover, our biomechanical model was not scaled according to subjects' body measurements, resulting in an additional source of error when compared to the Xsens' system, which considers it.

Field results show greater differences between joint angles data of systems than laboratory results. Although we used Xsens' data to compare with our data and assess both data consistency and agreement, note that there is no evidence in the literature about Xsens' system motion tracking performance in long-term acquisition within real industrial

TABLE 5. Laboratory and field reliability study results. ICC, 95% IC and SEM (°) values for each joint flexion/extension DoF data. The values are significant, with a p-value < 0.01.

	ICC		SEM (°)		95 % CI	
Joint	Laboratory	Field	Laboratory	Field	Laboratory	Field
Spine (Lumbar)	0,91	0,66	5,56	10,32	[0,89; 0,93]	[0,60; 0,71]
Left Shoulder	0,83	0,53	12,53	25,50	[0,79; 0,86]	[0,45; 0,60]
Left Elbow	0,94	0,58	7,74	20,19	[0,92; 0,95]	[0,51; 0,64]
Left Wrist	0,90	0,27	6,28	23,39	[0,88; 0,92]	[0,15; 0,38]
Right Shoulder	0,84	0,52	12,63	25,79	[0,80; 0,87]	[0,44; 0,59]
Right Elbow	0,95	0,62	6,63	19,39	[0,94; 0,96]	[0,55; 0,67]
Right Wrist	0,76	0,40	8,82	23,13	[0,70; 0,81]	[0,30; 0,49]
MEAN	0,88	0,51	8,60	21,10		

TABLE 6. Abbreviations used to refer to EAWS postures.

Posture	Abbreviation
Standing upright	U
Bent forward (20-60°)	BF
Strongly bent forward (>60°)	BS
Upright with elbow at/above shoulder level through arm flexion	FlexOS
Upright with hands above head level	OH

environments. The validations reported in the literature are collected in laboratory or controlled simulations of manufacturing processes settings [63]–[65]. This fact results from the difficulty of implementing inertial systems validation protocols with optical systems in real assembly lines. The increased data differences are due to issues that can affect both systems, such as the occurrence of magnetic interferences [66], [67]; longer acquisition time (i.e., 15-50 minutes) that can result in gyroscope sensor data drift over time; the occurrence of STA in a larger extent; and additional unknown independent variables that arise in real industrial settings, namely sensors displacements. Moreover, higher values of SEM in field also suggest a variability of the errors within each acquisition data, which can be due to the complexity and duration of the tasks.

Notice that, as described in section II-D, only DoF estimates from spine, shoulders, and elbows are used as input to the automated risk assessment. These estimates were taken as they showed moderate consistency with the Xsens' MoCap system. Moreover, further posture evaluation commits angular data quantization, as it was mentioned in section III-B, and angular ranges are wider, which do not enforce exact angle joint estimates.

B. POSTURE EVALUATION

1) WORKSTATION-LEVEL

The workstation-level analysis focuses on comparing the results among different workstations. Fig. 9 heatmaps depict the percentage of work-cycle in postures, i.e., biomechanical exposure, and the related risk score. The score scale was selected from 0 to 30 because the assigned values are within this range. Nevertheless, it should be noted that the interval of values considered for the assignment depends on the posture assessed, and it can reach a 100 score for the "upright with hands above head level" (OH) posture. The abbreviations used for postures are depicted in Table 6.

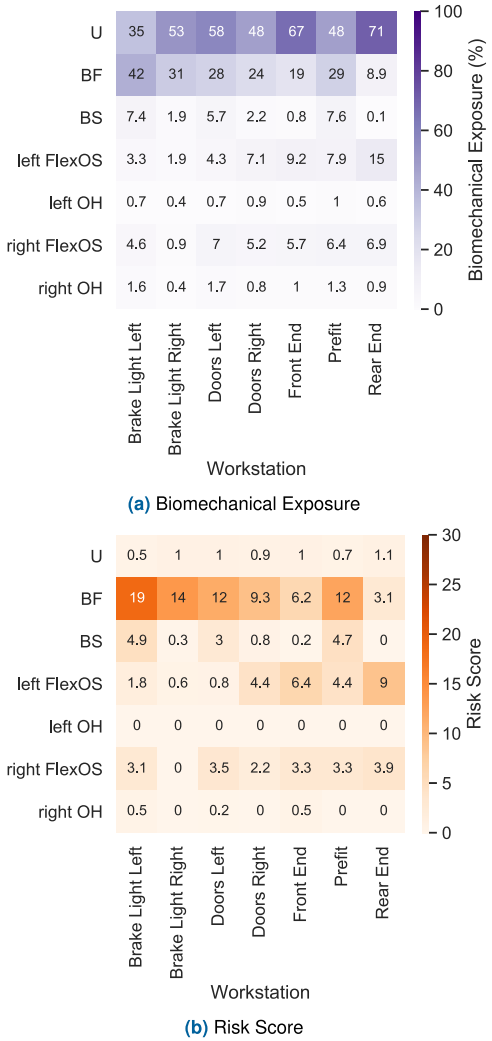

FIGURE 9. Workstation-level biomechanical exposure (top) and risk score (bottom). Biomechanical exposure results are reported as the mean of percentage of work-cycle time in each EAWS posture, while the risk score is a dimensionless measurement and linearly related to the biomechanical exposure.

The biomechanical exposure over the postures varies among workstations. For almost every workstation, the posture with the highest exposure is standing upright (U), followed by bent forward (BF), excluding *brake light* left, which is the opposite. Regarding strongly bent forward (BS), it can

be seen that the workstations of *prefit* and *brake light* left have a higher risk exposure value when compared to the other workstations.

Regarding the upper arms postures, some observations may be noted. Within *doors* fitting processes, the operators often perform the arm flexion at/above shoulder level (FlexOS) with the arm of the opposite side of the alignment, rather than the corresponding side (i.e., *doors* left present a higher percentage for right arm FlexOS, and vice-versa). Note that the *doors* fitting processes left and right are alike, but reversed. Operators support their bodies in the vehicle using the opposite arm flexed against it during the *doors*' fittings. Almost all of the remaining workstations show an exposure slightly higher to the left upper limb postures.

Prefit shows a positive exposure to all postures. *Front* and *rear end* workstations show only relevant exposure to arms FlexOS; *rear end* shows higher values for both arms than the *front end*, as it is bilateral and compromises both arms flexion to reach the *rear end* of the tailgate. Contrary to *doors* alignments, *brake light*s' are not alike; they complement each other.

By analyzing the risk scores and comparing them with the respective exposure percentages, we showed that the risk score assigned highly depends on the postures. For example, the longer the operator stands in the U posture, the lesser the risk of performing the fitting process because BF and BS postures result in a greater risk than U. In fact, notice that just standing at the U posture over the work-cycle time represents the optimal condition, that contributes to the lowest total risk score.

Generally, BF represents the greater risk scores, followed by BS for *prefit* and *brake light* left; then left arm FlexOS for right *doors*, *front* and *rear end*, and *prefit*; and right arm FlexOS for left *doors*, *front* and *rear end*, *prefit* and *brake light* left alignments. In the workstation-level perspective, *prefit* and *brake light* left have the highest calculated risk.

2) OPERATOR-LEVEL

The operator-level analysis aims to compare the biomechanical exposure and resulting risk between operators who conducted the same fitting process. Fig. 10 heatmaps depict the percentage of work-cycle in postures, and partials and total risk scores by workstation and operator. The discussion below considers body profiles from the operators (see Table 1).

- *Doors*: The working method performed by worker 1 is associated with the highest risk score for both *doors* fitting processes. Operator 1 also has the greatest profile among the subjects who performed the same workstations. Therefore, observing the exposure and risk score related to each posture, which contributes to the total risk score, it can be noted that the postures with higher demands are BF and BS for left *doors*, and BF and FlexOS for right *doors*. Regarding other operators, they have identical body profiles amongst each other. Nonetheless, operator 7 shows lower risk about BF and higher risk to both arms FlexOS.
- *Front End*: The results are similar among operators, besides their different body measurements. It is worth mentioning that operators 5 and 9 had high experience in the task, while operator 6 was still in a learning stage. However, no further reasoning can be provided within the scope of this study.
- *Prefit*: Operators 4 and 8 show similar total risk scores, higher than operator 5, who was an expert on *prefit*. In terms of body measurements, operator 5 has the smallest measures, while operator 4 has larger measures than the others. Analyzing the exposure and risk, higher values are reported to operator 4 regarding BF and left arm FlexOS compared with operator 8. Higher exposure and risk score to BS and right arm FlexOS postures are reported to operator 8.
- *Rear End*: Operator 5 results report the highest total risk score, and he has the smallest body profile. Operator 6 had a lower total risk score than operator 5. Both operators 5 and 6 seem to perform symmetric arms FlexOS. However, operator 5 does it to a greater extent during the work-cycle, probably due to the operator 6 qualification as a worker still in the learning process (observing and not doing some of the workstation's tasks). Plus, operator 5 performed BF more than the other workers, contributing to the higher total risk score. Operator 9 has a medium body profile, and he had an improved work method compared to operator 5.
- *Brake Lights*: Concerning *brake light* left, operator 8 presents the highest total risk score, followed by operator i5 and then operator 4. Operators 8 and 5 are smaller than operator 4 concerning their body measurements. Moreover, observing the exposure and risk, for operator 8, the highest values are for BF and BS, and, for operator 5, they are realized for BF. Regarding *brake light* right, operator 5 has the highest overall risk score due to high exposure to BF posture. Operator 8 displays a relevant risk score associated with BF, but not to other postures.

Additionally, we note that the arms OH posture is not often present, and U takes a considerable percentage of the work-cycle, which is desirable, as U is considered a less dangerous posture.

3) SYSTEMS DIFFERENCES

In order to study the differences in posture evaluation between data provided by the two inertial systems, Fig. 11 shows the absolute differences means and standard deviations of biomechanical exposure and risk score results for each EAWS posture.

As it can be seen, differences in biomechanical exposures and risk scores are greater concerning to postures that highly depended on the lumbar flexion/extension (i.e, U, BF), when compared with other postures.

Although joint angles retrieved by the systems were significantly different in field settings, in general, Fig. 11 shows that there is small differences between the posture risk score

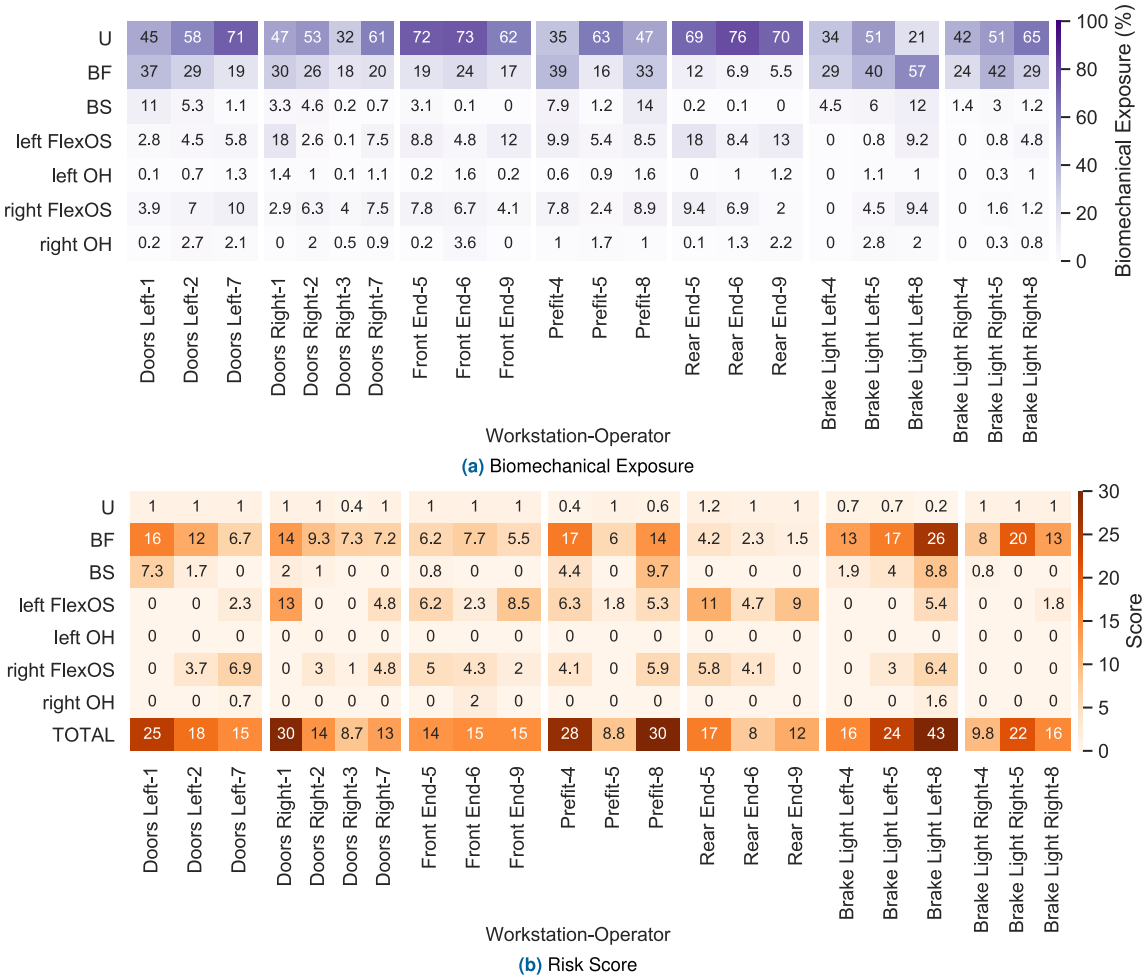

FIGURE 10. Operator-level biomechanical exposure (top) and risk score (bottom). Biomechanical exposure results are reported as the mean of percentage of work-cycle time in which each EAWS posture, while the risk score is a dimensionless measurement and linearly related to the biomechanical exposure.

results, excluding results concerning to BF posture. Notice that, in spite of U posture shows high differences respecting biomechanical exposure results, differences between the posture risk score results are minor when compared to other postures, which can be due to the low risk scores associated with that posture.

Nevertheless, there is a variation between subjects and tasks captured by standard deviations, which can be a result of a heterogeneous sensors placement or displacement during the acquisition, and subjects and tasks variability, besides the issues pointed out in Section III-A.

Despite the systems' angular estimates differences, the systems' evaluation results differences are not high, because the risk assessment uses angular estimates divided into angular ranges as input.

In contrast to prior studies [21], [29], [30], [42], [43] that used IMUs to track human motion and joint angle data as inputs for automated risk assessment based on ergonomic instruments, mainly RULA, we conducted a posture evaluation in an automotive assembly line, giving the developed methods a real-world application. Moreover, we conducted an operator-level analysis which revealed relevant differences in operators' work methods that might be related to their anthropometry characteristics. Those differences are reflected in the risk assessment results. Hence, the results of the operator-level analysis should be considered when redesigning fitting processes.

C. LIMITATIONS

The quantitative results reported herein should be considered in light of some limitations.

The sample dimension of the field trials is too small and, under these conditions, it might be improper to generalize the results regarding the evaluation (Section III-B). Only two to four operators with different body profiles were tracked by workstation. Plus, a sample size closer to the total population size would enable a statistical analysis of variables correlation and cause-effect on the posture evaluation.

The kinematic model used [55] lacks a detailed description of the upper body motion (e.g. the trunk flexion/extension

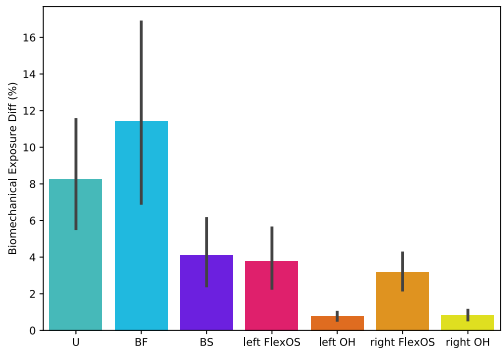

(a) Biomechanical Exposure

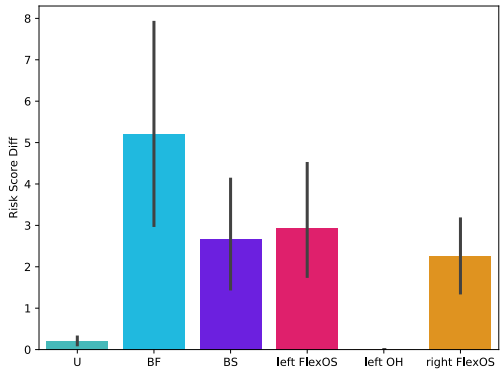

(b) Risk Score

FIGURE 11. Means and standard deviations of absolute differences between inertial systems results – operators' measurements of biomechanical exposure or risk score for each EAWS posture. A total of 22 measurements were considered.

varies between −90° and 90°) which might have resulted in errors in the joint angles estimates while users performed extreme upper body segments postures and/or highly dynamic movements. Generally, these errors were characterized by a clipping of the segment estimates at their maximum value, and there seems to exist some error propagation to the adjacent segment estimates.

On the other hand, a set of reduced body measurements were collected. The collection of more upper body segments anthropometric measurements would be relevant to provide a feasible relationship between upper body posture and risk.

IV. CONCLUSION

We provided a comprehensive study of an automatic approach to evaluate posture biomechanical exposure and risk in industrial contexts, focusing on a case study of an automotive assembly line. We proposed an on-body sensor network of inertial sensors, a motion tracking framework used to reconstruct upper body joints movement on the sagittal plane, and an automated approach to calculate EAWS scores for basic positions and postures of the trunk and arm movements. We compared our results with a commercial system in laboratory and field trials.

The comparison results showed that within laboratory settings, the motion tracking estimates consistency (ICC = 0,88) and agreement (SEM = 8,60°) are good. Nevertheless, these differences between systems data fairly increased for automotive assembly line acquisitions (ICC = 0,51; SEM = 21,10°). The reasons can be magnetic field disturbances, STA and sensor displacement occurrences, and using a low complexity biomechanical model to describe upper body motion.

Though we considered field joint angle data reliable for the risk assessment as exact estimates were not required for the application; further experiments will be carried out to extensively validate our MoCap inertial system and motion tracking framework.

Regarding the evaluation, workstation-level results showed that the riskier workstations are *prefit* and *brake light* left with high contributions of BF and arms FlexOS postures. The operator-level analysis revealed quantitative differences among different operators performing the same task. We also identified some hypotheses that might explain these differences, namely the variations within body profiles and experience. Nevertheless, no generalizations concerning the fit shop's population can be provided as a separate study with a large population would be necessary.

The framework proposed in our study might be used as a tool to support risk assessment in industrial lines, providing quantitative insights about the actual exposure of workstations and operators. This framework can also be used as an asset to support operator training and evaluate the effectiveness of ergonomic interventions.

A. FUTURE WORK

This study leaves some unsolved problems and opens new research questions to which we will be devoting additional research effort in the future.

Data collection with a larger sample size could be conducted in the field to provide population-representative relationships between risk assessment outputs and participants' body measurements.

A continuous enhancement of the motion tracking framework should be pursued. Particularly, the system should be validated with an optical MoCap system. Moreover, we may have failed on upper body segments' motion estimation regarding extreme segments' postures using a low complexity biomechanical model. In the future, using a more complex upper body model can be a valuable alternative to obtain better DoFs angular estimates for extreme positions and contribute towards more accurate motion tracking.

Our data analysis focused on implementing an approach to evaluate static postures according to EAWS. Nevertheless, there exist other quantitative means of assessing biomechanical exposures which might be interesting to complete the current analysis, such as evaluating the dimensions of intensity, repetition, and duration [9]. Data mining time series methods might be used to calculate these variables and provide further insights.

ACKNOWLEDGMENT

The authors would like to thank technical support from the OpenSim software development team of Stanford University,

and also would like to thank Johanna O'Day, Ayman Habib, and Scott Uhlrich for valuable feedback and discussions regarding the OpenSense pipeline.

REFERENCES

[1] J. de Kok, P. Vroonhof, J. Snijders, G. Roullis, M. Clarke, K. Peereboom, P. van Dorst, and I. Isusi. (2019). *Summary—Work-Related Musculoskeletal Disorders: Prevalence, Costs and Demographics in the EU*. OSHA European Agency for Safety and Health at Work. [Online]. Available: https://osha.europa.eu/pt/publications/summary-work-related-musculoskeletal-disorders-prevalence-costs-and-demographics-eu

[2] O. Korhan and A. A. Memon. (Mar. 2019). *Work-Related Musculoskeletal Disorders*. [Online]. Available: https://www.intechopen.com/chapters/66431

[3] Z. Whysall, J. Bowden, and M. Hewitt, "Sickness presenteeism: Measurement and management challenges," *Ergonomics*, vol. 61, no. 3, pp. 341–354, Mar. 2018, doi: 10.1080/00140139.2017.1365949.

[4] T. R. Hales and B. P. Bernard, "Epidemiology of work-related musculoskeletal disorders," *Orthopedic Clinics North Amer.*, vol. 4, pp. 679–709, Oct. 1996. [Online]. Available: https://pubmed.ncbi.nlm.nih.gov/8823390/

[5] C. Berlin and C. Adams, *Production Ergonomics: Designing Work Systems to Support Optimal Human Performance*. London, U.K.: Ubiquity Pres, Jun. 2017, ch. 1. [Online]. Available: http://www.ubiquitypress.com/site/books/10.5334/bbe/read/

[6] R. Ellegast, K. Deroiste V. Klaus, and R. Kluser. (May 2020). *Assessment of Physical Workloads to Prevent Work-Related MSDs*. OSHWiki. [Online]. Available: https://oshwiki.eu/wiki/Assessment_of_physical_workloads_to_prevent_work-related_MSDs

[7] B. D. Lowe, P. G. Dempsey, and E. M. Jones, "Ergonomics assessment methods used by ergonomics professionals," *Appl. Ergonom.*, vol. 81, Nov. 2019, Art. no. 102882, doi: 10.1016/j.apergo.2019.102882.

[8] K. Schaub, G. Caragnano, B. Britzke, and R. Bruder, "The European assembly worksheet," *Theor. Issues Ergonom. Sci.*, vol. 14, no. 6, pp. 616–639, Nov. 2013, doi: 10.1080/1463922x.2012.678283.

[9] D. H. Seidel, D. M. Ditchen, U. M. Hoehne-Hückstädt, M. A. Rieger, and B. Steinhilber, "Quantitative measures of physical risk factors associated with work-related musculoskeletal disorders of the elbow: A systematic review," *Int. J. Environ. Res. Public Health*, vol. 16, no. 1, p. 130, Jan. 2019, doi: 10.3390/ijerph16010130.

[10] P. J. Keir, A. Farias Zuniga, D. M. Mulla, and K. G. Somasundram, "Relationships and mechanisms between occupational risk factors and distal upper extremity disorders," *Hum. Factors, J. Hum. Factors Ergonom. Soc.*, vol. 63, no. 1, pp. 5–31, Feb. 2021, doi: 10.1177/0018720819860683.

[11] D. Romero, J. Stahre, T. Wuest, O. Noran, P. Bernus, Å. Fast-Berglund, and D. Gorecky, "Towards an operator 4.0 typology: A human-centric perspective on the fourth industrial revolution technologies," in *Proc. CIE*, Oct. 2016, pp. 29–31. [Online]. Available: https://www.researchgate.net/publication/309609488_Towards_an_Operator_40_Typology_A_Human-Centric_Perspective_on_the_Fourth_Industrial_Revolution_Technologies

[12] M. Menolotto, D.-S. Komaris, S. Tedesco, B. O'Flynn, and M. Walsh, "Motion capture technology in industrial applications: A systematic review," *Sensors*, vol. 20, no. 19, p. 5687, Oct. 2020.

[13] S. Lim and C. D'Souza, "A narrative review on contemporary and emerging uses of inertial sensing in occupational ergonomics," *Int. J. Ind. Ergonom.*, vol. 76, Mar. 2020, Art. no. 102937, doi: 10.1016/j.ergon.2020.102937.

[14] X. Zhang, M. C. Schall, H. Chen, S. Gallagher, G. A. Davis, and R. Sesek, "Manufacturing worker perceptions of using wearable inertial sensors for multiple work shifts," *Appl. Ergonom.*, vol. 98, Jan. 2022, Art. no. 103579, doi: 10.1016/j.apergo.2021.103579.

[15] M. Nazarahari and H. Rouhani, "40 years of sensor fusion for orientation tracking via magnetic and inertial measurement units: Methods, lessons learned, and future challenges," *Inf. Fusion*, vol. 68, pp. 67–84, Apr. 2021, doi: 10.1016/j.inffus.2020.10.018.

[16] A. Filippeschi, N. Schmitz, M. Miezal, G. Bleser, E. Ruffaldi, and D. Stricker, "Survey of motion tracking methods based on inertial sensors: A focus on upper limb human motion," *Sensors*, vol. 17, no. 6, p. 1257, Jun. 2017. [Online]. Available: http://www.mdpi.com/1424-8220/17/6/1257

[17] M. Al Borno, J. O'Day, V. Ibarra, J. Dunne, A. Seth, A. Habib, C. Ong, J. Hicks, S. Uhlrich, and S. Delp, "OpenSense: An open-source toolbox for inertial-measurement-unit-based measurement of lower extremity kinematics over long durations," *J. NeuroEngineering Rehabil.*, vol. 19, Dec. 2022, Art. no. 22. [Online]. Available: https://www.biorxiv.org/content/early/2021/07/02/2021.07.01.450788.full.pdf

[18] B. Pedro, S. Cabral, and A. P. Veloso, "Concurrent validity of an inertial measurement system in tennis forehand drive," *J. Biomechanics*, vol. 121, May 2021, Art. no. 110410, doi: 10.1016/j.jbiomech.2021.110410.

[19] I. Weygers, M. Kok, H. De Vroey, T. Verbeerst, M. Versteyhe, H. Hallez, and K. Claeys, "Drift-free inertial sensor-based joint kinematics for long-term arbitrary movements," *IEEE Sensors J.*, vol. 20, no. 14, pp. 7969–7979, Mar. 2020, doi: 10.1109/jsen.2020.2982459.

[20] C. Huang, W. Kim, Y. Zhang, and S. Xiong, "Development and validation of a wearable inertial sensors-based automated system for assessing work-related musculoskeletal disorders in the workspace," *Int. J. Environ. Res. Public Health*, vol. 17, no. 17, p. 6050, Aug. 2020, doi: 10.3390/ijerph17176050.

[21] S. Santos, D. Folgado, J. Rodrigues, N. Mollaei, C. Fujão, and H. Gamboa, "Explaining the ergonomic assessment of human movement in industrial contexts," in *Proc. 13th Int. Conf. Biomed. Eng. Syst. Technol.*, 2020, pp. 79–88, doi: 10.5220/0008953800790088.

[22] B. Bouvier, S. Duprey, L. Claudon, R. Dumas, and A. Savescu, "Upper limb kinematics using inertial and magnetic sensors: Comparison of sensor-to-segment calibrations," *Sensors*, vol. 15, no. 8, pp. 18813–18833, Jul. 2015, doi: 10.3390/s150818813.

[23] M. Peruzzini, F. Grandi, S. Cavallaro, and M. Pellicciari, "Using virtual manufacturing to design human-centric factories: An industrial case," *Int. J. Adv. Manuf. Technol.*, vol. 115, no. 3, pp. 873–887, Jul. 2021, doi: 10.1007/s00170-020-06229-2.

[24] S. A. Ferguson, W. S. Marras, W. Gary Allread, G. G. Knapik, K. A. Vandlen, R. E. Splittstoesser, and G. Yang, "Musculoskeletal disorder risk as a function of vehicle rotation angle during assembly tasks," *Appl. Ergonom.*, vol. 42, no. 5, pp. 699–709, Jul. 2011, doi: 10.1016/j.apergo.2010.11.004.

[25] G.-Å. Hansson, I. Balogh, K. Ohlsson, L. Granqvist, C. Nordander, I. Arvidsson, I. Åkesson, J. Unge, R. Rittner, U. Strömberg, and S. Skerfving, "Physical workload in various types of work: Part II. Neck, shoulder and upper arm," *Int. J. Ind. Ergonom.*, vol. 40, no. 3, pp. 267–281, May 2010, doi: 10.1016/j.ergon.2009.11.002.

[26] M. Acuna and A. R. Karduna, "Wrist activity monitor counts are correlated with dynamic but not static assessments of arm elevation exposure made with a triaxial accelerometer," *Ergonomics*, vol. 55, no. 8, pp. 963–970, Aug. 2012, doi: 10.1080/00140139.2012.676672.

[27] T. Möller, S. E. Mathiassen, H. Franzon, and S. Kihlberg, "Job enlargement and mechanical exposure variability in cyclic assembly work," *Ergonomics*, vol. 47, no. 1, pp. 19–40, Jan. 2004, doi: 10.1080/0014013032000121651.

[28] J. Santos, A. B. Abreu, P. Fonseca, C. Carvalhais, J. S. Baptista, R. Santos, and M. Vaz, "Influence of automation on biomechanical exposure of the upper-limbs in an industrial assembly line: A pilot study," *Int. J. Occupational Environ. Saf.*, vol. 4, no. 2, pp. 1–11, Nov. 2020, doi: 10.24840/2184-0954_004.002_0001.

[29] D. Álvarez, J. C. Alvarez, R. C. González, and A. M. López, "Upper limb joint angle measurement in occupational health," *Comput. Methods Biomechanics Biomed. Eng.*, vol. 19, no. 2, pp. 159–170, Jan. 2016, doi: 10.1080/10255842.2014.997718.

[30] N. Vignais, M. Miezal, G. Bleser, K. Mura, D. Gorecky, and F. Marin, "Innovative system for real-time ergonomic feedback in industrial manufacturing," *Appl. Ergonom.*, vol. 44, no. 4, pp. 566–574, Jul. 2013, doi: 10.1016/j.apergo.2012.11.008.

[31] D. Folgado, M. Barandas, R. Matias, R. Martins, M. Carvalho, and H. Gamboa, "Time alignment measurement for time series," *Pattern Recognit.*, vol. 81, pp. 268–279, Sep. 2018, doi: 10.1016/j.patcog.2018.04.003.

[32] D. M. Folgado, M. Barandas, and M. A. Carvalho, and H. F. Gamboa. (Feb. 2020). *Method and Devive for Assessing Physical Movement of an Operator During a Work Cycle Execution on an Manufacturing Work Station*. [Online]. Available: https://worldwide.espacenet.com/patent/search/family/067211511/publication/EP3758023B1?q=pn%3DEP3758023B1

[33] P. Matias, D. Folgado, H. Gamboa, and A. Carreiro, "Time series segmentation using neural networks with cross-domain transfer learning," *Electronics*, vol. 10, no. 15, p. 1805, Jul. 2021, doi: 10.3390/electronics10151805.
[34] P. Matias, D. Folgado, H. Gamboa, and A. Carreiro, "Robust anomaly detection in time series through variational AutoEncoders and a local similarity score," in *Proc. 14th Int. Conf. Biomed. Eng. Syst. Technol.*, 2021, pp. 91–102, doi: 10.5220/0010320500910102.
[35] J. Zhao and E. Obonyo, "Applying incremental deep neural networks-based posture recognition model for ergonomics risk assessment in construction," *Adv. Eng. Informat.*, vol. 50, Oct. 2021, Art. no. 101374, doi: 10.1016/j.aei.2021.101374.
[36] A. Malaise, P. Maurice, F. Colas, and S. Ivaldi, "Activity recognition for ergonomics assessment of industrial tasks with automatic feature selection," *IEEE Robot. Autom. Lett.*, vol. 4, no. 2, pp. 1132–1139, Apr. 2019, doi: 10.1109/lra.2019.2894389.
[37] J. Anderson, M. H. Granat, A. E. Williams, and C. Nester, "Exploring occupational standing activities using accelerometer-based activity monitoring," *Ergonomics*, vol. 62, no. 8, pp. 1055–1065, Aug. 2019, doi: 10.1080/00140139.2019.1615640.
[38] M. Brandt, P. Madeleine, A. Samani, M. D. Jakobsen, S. Skals, J. Vinstrup, and L. L. Andersen, "Accuracy of identification of low or high risk lifting during standardised lifting situations," *Ergonomics*, vol. 61, no. 5, pp. 710–719, May 2018, doi: 10.1080/00140139.2017.1408857.
[39] S. M. Hosseinian, Y. Zhu, R. K. Mehta, M. Erraguntla, and M. A. Lawley, "Static and dynamic work activity classification from a single accelerometer: Implications for ergonomic assessment of manual handling tasks," *IISE Trans. Occupational Ergonom. Hum. Factors*, vol. 7, no. 1, pp. 59–68, Jan. 2019, doi: 10.1080/24725838.2019.1608873.
[40] R. Varandas, D. Folgado, and H. Gamboa, "Evaluation of spatial-temporal anomalies in the analysis of human movement," in *Proc. 12th Int. Joint Conf. Biomed. Eng. Syst. Technol.*, 2019, pp. 163–170, doi: 10.5220/0007386701630170.
[41] S. Kim and M. A. Nussbaum, "An evaluation of classification algorithms for manual material handling tasks based on data obtained using wearable technologies," *Ergonomics*, vol. 57, no. 7, pp. 1040–1051, Jul. 2014, doi: 10.1080/00140139.2014.907450.
[42] A. Villalobos and A. M. Cawley, "Prediction of slaughterhouse workers' RULA scores and knife edge using low-cost inertial measurement sensor units and machine learning algorithms," *Appl. Ergonom.*, vol. 98, Jan. 2022, Art. no. 103556, doi: 10.1016/j.apergo.2021.103556.
[43] L. Peppoloni, A. Filippeschi, E. Ruffaldi, and C. A. Avizzano, "A novel wearable system for the online assessment of risk for biomechanical load in repetitive efforts," *Int. J. Ind. Ergonom.*, vol. 52, pp. 1–11, Mar. 2016, doi: 10.1016/j.ergon.2015.07.002.
[44] X. Ji and D. Piovesan, "RETRACTED: Validation of inertial-magnetic wearable sensors for full-body motion tracking of automotive manufacturing operations," *Int. J. Ind. Ergonom.*, vol. 79, Sep. 2020, Art. no. 103005, doi: 10.1016/j.ergon.2020.103005.
[45] C. Maurer-Grubinger, F. Holzgreve, L. Fraeulin, W. Betz, C. Erbe, D. Brueggmann, E. M. Wanke, A. Nienhaus, D. A. Groneberg, and D. Ohlendorf, "Combining ergonomic risk assessment (RULA) with inertial motion capture technology in dentistry—Using the benefits from two worlds," *Sensors*, vol. 21, no. 12, p. 4077, Jun. 2021, doi: 10.3390/s21124077.
[46] Xsens. (2022). *Xsens.com*. [Online]. Available: https://www.xsens.com/hubfs/Downloads/usermanual/MVN_User_Manual.pdf
[47] T. Baur. (2021). *NOVA Documentation*. Rawgit.com. [Online]. Available: https://rawgit.com/hcmlab/nova/master/docs/index.html
[48] H. Zhou and H. Hu, "Inertial sensors for motion detection of human upper limbs," *Sensor Rev.*, vol. 27, no. 2, pp. 151–158, 2007, doi: 10.1108/02602280710731713.
[49] M. M. Hassan, M. Z. Uddin, A. Mohamed, and A. Almogren, "A robust human activity recognition system using smartphone sensors and deep learning," *Future Gener. Comput. Syst.*, vol. 81, pp. 307–313, Apr. 2018, doi: 10.1016/j.future.2017.11.029.
[50] J. He, C. Sun, and P. Wang, "Noise reduction for MEMS gyroscope signal: A novel method combining ACMP with adaptive multiscale SG filter based on AMA," *Sensors*, vol. 19, no. 20, p. 4382, Oct. 2019, doi: 10.3390/s19204382.
[51] T. R. Bennett, N. Gans, and R. Jafari, "Data-driven synchronization for Internet-of-Things systems," *ACM Trans. Embedded Comput. Syst.*, vol. 16, no. 3, pp. 1–24, Jul. 2017, doi: 10.1145/2983627.
[52] M. Garcia. (2021). *Attitude and Heading Reference Systems*. GitHub. [Online]. Available: https://ahrs.readthedocs.io/en/latest/
[53] S. Madgwick. (Apr. 2010). *An Efficient Orientation Filter for Inertial and Inertial Magnetic Sensor Arrays*. [Online]. Available: http://www.x-io.co.uk/open-source-imu-and-ahrs-algorithms/
[54] J. B. Kuipers. *Quaternions and Rotation Sequences: A Primer with Applications to Orbits, Aerospace and Virtual Reality*. Princeton, NJ, USA: Princeton Univ. Press, 2020, ch. 5, pp. 103–140, doi: 10.1515/9780691211701-008.
[55] A. Rajagopal, C. L. Dembia, M. S. DeMers, D. D. Delp, J. L. Hicks, and S. L. Delp, "Full-body musculoskeletal model for muscle-driven simulation of human gait," *IEEE Trans. Biomed. Eng.*, vol. 63, no. 10, pp. 2068–2079, Oct. 2016, doi: 10.1109/tbme.2016.2586891.
[56] A. Seth, R. Matias, A. P. Veloso, and S. L. Delp, "A biomechanical model of the scapulothoracic joint to accurately capture scapular kinematics during shoulder movements," *PLoS ONE*, vol. 11, no. 1, Jan. 2016, Art. no. e0141028, doi: 10.1371/journal.pone.0141028.
[57] S. Williams, R. Schmidt, C. Disselhorst-Klug, and G. Rau, "An upper body model for the kinematical analysis of the joint chain of the human arm," *J. Biomechanics*, vol. 39, no. 13, pp. 2419–2429, Jan. 2006, doi: 10.1016/j.jbiomech.2005.07.023.
[58] K. R. S. Holzbaur, W. M. Murray, and S. L. Delp, "A model of the upper extremity for simulating musculoskeletal surgery and analyzing neuromuscular control," *Ann. Biomed. Eng.*, vol. 33, no. 6, pp. 829–840, 2005, doi: 10.1007/s10439-005-3320-7.
[59] T. K. Koo and M. Y. Li, "A guideline of selecting and reporting intraclass correlation coefficients for reliability research," *J. Chiropractic Med.*, vol. 15, no. 2, pp. 155–163, 2016, doi: 10.1016/j.jcm.2016.02.012.
[60] G. Atkinson and A. M. Nevill, "Statistical methods for assessing measurement error (reliability) in variables relevant to sports medicine," *Sports Med.*, vol. 26, no. 4, pp. 217–238, 1998, doi: 10.2165/00007256-199826040-00002.
[61] M. Zabat, A. Ababou, N. Ababou, and R. Dumas, "IMU-based sensor-to-segment multiple calibration for upper limb joint angle measurement—A proof of concept," *Med. Biol. Eng. Comput.*, vol. 57, no. 11, pp. 2449–2460, Nov. 2019, doi: 10.1007/s11517-019-02033-7.
[62] A. Carnevale, U. G. Longo, E. Schena, C. Massaroni, D. Lo Presti, A. Berton, V. Candela, and V. Denaro, "Wearable systems for shoulder kinematics assessment: A systematic review," *BMC Musculoskeletal Disorders*, vol. 20, Dec. 2019, Art. no. 546, doi: 10.1186/s12891-019-2930-4.
[63] L. De Baets, S. Vanbrabant, C. Dierickx, R. van der Straaten, and A. Timmermans, "Assessment of scapulothoracic, glenohumeral, and elbow motion in adhesive capsulitis by means of inertial sensor technology: A within-session, intra-operator and inter-operator reliability and agreement study," *Sensors*, vol. 20, no. 3, p. 876, Feb. 2020, doi: 10.3390/s20030876.
[64] X. Robert-Lachaine, H. Mecheri, C. Larue, and A. Plamondon, "Validation of inertial measurement units with an optoelectronic system for whole-body motion analysis," *Med. Biol. Eng. Comput.*, vol. 55, no. 4, pp. 609–619, Apr. 2017, doi: 10.1007/s11517-016-1537-2.
[65] X. Robert-Lachaine, H. Mecheri, A. Müller, C. Larue, and A. Plamondon, "Validation of a low-cost inertial motion capture system for whole-body motion analysis," *J. Biomechanics*, vol. 99, Jan. 2020, Art. no. 109520, doi: 10.1016/j.jbiomech.2019.109520.
[66] X. Robert-Lachaine, H. Mecheri, C. Larue, and A. Plamondon, "Effect of local magnetic field disturbances on inertial measurement units accuracy," *Appl. Ergonom.*, vol. 63, pp. 123–132, Sep. 2017, doi: 10.1016/j.apergo.2017.04.011.
[67] W. H. K. de Vries, H. E. J. Veeger, C. T. M. Baten, and F. C. T. van der Helm, "Magnetic distortion in motion labs, implications for validating inertial magnetic sensors," *Gait Posture*, vol. 29, no. 4, pp. 535–541, Jun. 2009. [Online]. Available: https://research.vu.nl/en/publications/magnetic-distortion-in-motion-labs-implications-for-validating-in

MARIA LUA NUNES received the M.Sc. degree in biomedical and biophysics engineering from the Faculdade de Ciências of University of Lisbon (FCUL), in 2021. During her academic path, she attended an exchanging module of the European Institute of Innovation and Technology, Advanced Quantitative Methods in Healthcare Innovation, Copenhagen, Denmark. She also did several short-term internships in Portugal and abroad. She is currently a Researcher of the Fraunhofer Center for Assistive Information and Communication Solutions (AICOS), Intelligent Systems Group. Her research interests include motion reconstruction, mainly using kinematics and kinetics modeling, and analysis.

DUARTE FOLGADO received the M.Sc. degree in biomedical engineering from the Faculdade de Ciências e Tecnologia, NOVA University of Lisbon (FCT NOVA), in 2015. He is currently pursuing the Ph.D. degree in biomedical engineering. Since 2015, he been working as a Scientist with the Fraunhofer Portugal Research Center for Assistive Information and Communication Solutions (AICOS) on the intelligent systems team. His research interests include signal processing, data mining, machine learning, and explainable artificial intelligence applied to time series.

CARLOS FUJÃO received the bachelor's and master's degrees in ergonomics from the Faculty of Human Kinetics, Technical University of Lisbon, Portugal. He has been working in the automotive industry, since 1998, as an Ergonomist. He is currently working at Volkswagen Autoeuropa, Palmela, Portugal. His main activities are related to topics, such as ergonomics risk assessment, ergonomics intervention for working conditions improvements, and risk exposure management to repetitive and manual material handling tasks. He is also responsible for boosting research projects regarding ergonomic topics, being the Tutor for Ph.D. student's. From 2003 to 2009, he was the Chairperson of the Portuguese Ergonomics Association.

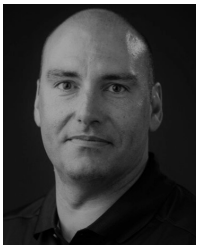

LUÍS SILVA received the Ph.D. degree in human kinetics from the Faculty of Human Motricity, University of Lisbon, in 2014. He is currently a Postdoctoral Researcher at LIBPhys, Faculdade de Ciências e Tecnologia, NOVA University of Lisbon (FCT NOVA) in the "Operator—Digital Transformation in Industry with a focus on the Operator 4.0," a supported Massachusetts Institute of Technology (MIT) Flagship Project. Previously, he was also a Postdoctoral Researcher with the Department of Biomechanics, University of Nebraska, Omaha, USA, awarded with a COBRE pilot project funded by the National Institutes of Health (NIH). He has a Doctoral Scholarship focused on machine learning applied to electromyography during his Ph.D. degree. His research interests include signal processing, nonlinear methods and variability, and artificial intelligence.

JOÃO RODRIGUES received the M.Sc. degree in biomedical engineering from the University of Coimbra, where he developed a strong attachment to optical and electronic instrumentation, and software development for signal processing, especially in the domain of parallel processing. He is currently pursuing the Ph.D. degree with the Faculdade de Ciências e Tecnologia, NOVA University of Lisbon (FCT NOVA), in the context of ergonomics, in partnership with Volkswagen Autoeuropa. Having always been in mind to bring novelty into this world, he decided to follow the path of research and development, which led him to the UNL, where he started his professional career as a Researcher at LIBPhys. His research interests include the development of new methodologies for pattern search, analysis, and generation in time series.

PEDRO MATIAS received the M.Sc. degree in biomedical engineering from the NOVA University School of Science and Technology, in 2021. He is currently working as a Scientist with the Intelligent Systems Group, Fraunhofer AICOS. He collaborates in projects, where the creation of intelligence from the available data can provide valuable solutions in response to their main challenges. His research interests include exploring machine learning and deep learning techniques for automatic knowledge extraction from time series, trying to bridge research and development areas to tackle real-world problems.

MARÍLIA BARANDAS received the M.Sc. degree in biomedical engineering from the Faculdade de Ciências e Tecnologia, NOVA University of Lisbon (FCT NOVA), in 2013, where she is currently pursuing the Ph.D. degree under the Biomedical Engineering Doctoral Program. She has been working with the Fraunhofer Center for Assistive Information and Communication Solutions (AICOS) as a Scientist, since 2015. Prior to joining AICOS, she was an Assistant Lecturer with the Electrical and Computer Engineering Department, FCT NOVA, and a Research Engineer with the Centre of Technology and Systems, Computational Intelligence Research Group. Her research interests include knowledge extraction, probability theory, machine learning, and explainable artificial intelligence.

ANDRÉ V. CARREIRO received the Ph.D. degree in biomedical engineering from Técnico Lisboa—University of Lisbon. He is currently a Senior Researcher of the Fraunhofer Center for Assistive Information and Communication Solutions (AICOS), Intelligent Systems Group. He has been applied machine learning techniques, since 2010, and he has been working with deep learning methods, since 2016, both in academia and industry, resulting in a balance between innovation and making sure, such techniques are applied efficiently to solve real-world problems, in areas from healthcare to security, and industry.

SARA MADEIRA received the M.Sc. degree in data science from the Faculty of Sciences of University of Lisbon (FCUL). She is currently an Associate Professor with the Department of Informatics, FCUL. She teaches courses on machine learning, data mining, foundations of data science, and introduction to research in data science. She is also a Senior Researcher at LASIGE, where she coordinates the Data and Systems Intelligence Research Line of Excellence (RLE), being a member of the Health and Biomedical Informatics RLE.

HUGO GAMBOA (Senior Member, IEEE) received the Ph.D. degree in electrical and computer engineering from the Instituto Superior Técnico of University of Lisbon (IST UL), in 2007. He co-founded and is the President of PLUX, a company that develops bio-signals monitoring wearable technology. He is currently a Researcher with the Laboratory for Instrumentation, Biomedical Engineering and Radiation Physics (LIBPhys), Faculdade de Ciências e Tecnologia, NOVA University of Lisbon (FCT NOVA), where he is also an Associate Professor with the Physics Department. Since 2014, he has been a Senior Researcher with the Fraunhofer Center for Assistive Information and Communication Solutions (AICOS). His research interests include bio-signals processing and instrumentation.